

---

## Structural Acoustics and Vibration (others): Paper ICA2016-570

### Material properties and microstructure contributions to vibrational damping in arundo donax L: Reed cane for woodwind instruments

Connor Kemp<sup>(a)</sup>, Gary Scavone<sup>(a)</sup>

<sup>(a)</sup> Computational Acoustic Modeling Laboratory, Centre for Interdisciplinary Research in Music Media and Technology, Music Technology, Schulich School of Music, McGill University, Montreal, Quebec, H3A 1E3 Canada, [connor.kemp@mail.mcgill.ca](mailto:connor.kemp@mail.mcgill.ca)

#### Abstract

Natural cane reeds (Latin name *Arundo Donax L* and here termed ADL) have been used on woodwind instruments for centuries with little change. The reed acts as a mechanical valve controlling the energy input into the musical instrument and it is the musician's first option for altering the instrument's sound and response characteristics. Despite this, their consistency, variable performance, durability and sensitivity to ambient conditions make it difficult for the musician to find and maintain a reed that responds to their liking. Manufacturers control the geometry of the reed to a high degree of repeatability, minimizing the influence of geometry on inter-reed variability. Thus it is desirable to examine the material, microstructural and anatomical properties of the reed and their contributions to vibrational performance. In the present work raw samples of ADL obtained from a manufacturer in pre-cut form are sectioned into longitudinal and transverse specimens for mechanical characterization in three primary directions. Measures of material damping (internal friction) are obtained through observations of phase lag between input stress and output strain waveforms. The effects of mechanically induced vibrations on these measurements are also investigated through the use of a shaker rig inducing small amplitude, fixed-free vibrations up to 1000Hz. Experimental samples are examined under optical microscope for characterization of several microstructural features. It is shown that the fiber size and specimen orientation contributes to the measured values of damping ( $\tan \delta$ ). Mechanical vibrations simulating in-vivo conditions are also found to affect  $\tan \delta$  values with time. Future work will include the comparison of the results with those obtained from reeds that are regularly played by a professional musician.

**Keywords:** material damping, material vibration, microstructure analysis, music, mechanics

---

---

# Material properties and microstructure contributions to vibrational damping in arundo donax L: Reed cane for woodwind instruments

## 1 Introduction

Reeds have been used on woodwind instruments in their current form for hundreds of years. The reed is extremely important to the performance and sound generated by the instrument as it acts as a mechanical valve controlling the volume flow of air into the air column. Natural cane reeds (Latin form *Arundo Donax L.*, or ADL) are desirable in terms of their vibrational response, although their inconsistent behaviour and durability are found to be problematic by musicians. It is also quite difficult to delineate the properties (vibrational, material and mechanical) that objectively form a “good” reed, and once found, a good quality reed can change with time. Before proper alternative materials possessing superior durability attributes can be selected, the most important material properties of ADL pertinent to vibrational behaviour must be determined. Therefore, it is desirable to simulate vibrational loads on raw ADL material such that potential changes in material damping properties can be identified and related to prevalent material properties.

## 2 Background

### 2.1 Reed loading

A component of the enigma that is woodwind reed performance is their variable behaviour. The relative influences of wetting-drying cycles and mechanical vibration on the reed’s lifespan are not well understood, despite these components constituting the majority of degradation mechanisms. The magnitudes of mechanical loads during simulated experimental conditions [1] and those during normal practice (in-vivo) are found to be on the order of 100 to 200MPa. The largest components of stress are localized to the tip of the reed where deflections are large relative to the thickness. Considering the reed geometry more specifically, the tip thickness of alto saxophone reeds is 100 microns or less. This is important as microstructural features of the ADL material are within the same order of magnitude. The sense of loading is also complex in nature, consisting of large tensile and compressive components, dependent on the playing frequency and applied embouchure pressure. A simplified setup of the loading conditions of a woodwind reed are considered in Figure 1, where the reed is mounted as a simple cantilevered beam with an additional distributed load close to the tip. This distributed load represents the lip of the musician and applies a time-varying force to the reed. In-vivo stress and strains are usually found to have larger relative compressive peaks and thus compressive testing was of primary interest in the present study.

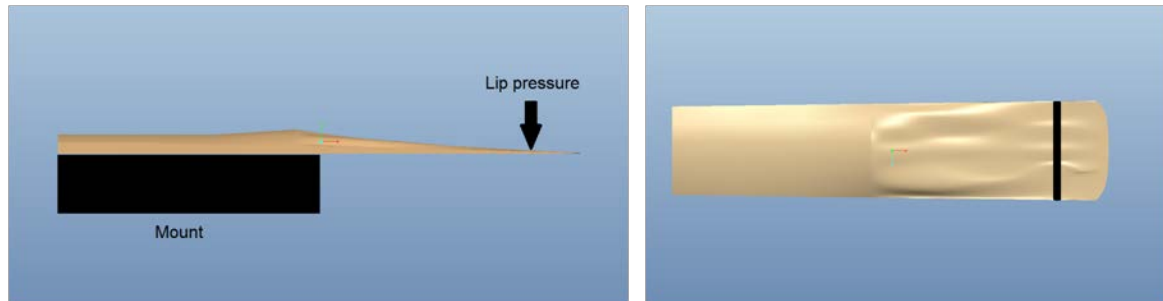


Figure 1: Alto saxophone reed with simplified loading conditions (left: side view, right: top view)

## 2.2 Arundo donax L.

Natural cane reeds used for woodwind instruments are constructed from ADL. ADL is a member of the grass family and shares many similarities with bamboo [2], [3]. At the microstructure level ADL contains a parenchyma matrix of porous material and fibrous, stiffening agents with a much higher density. These main features are shown in Figure 2.

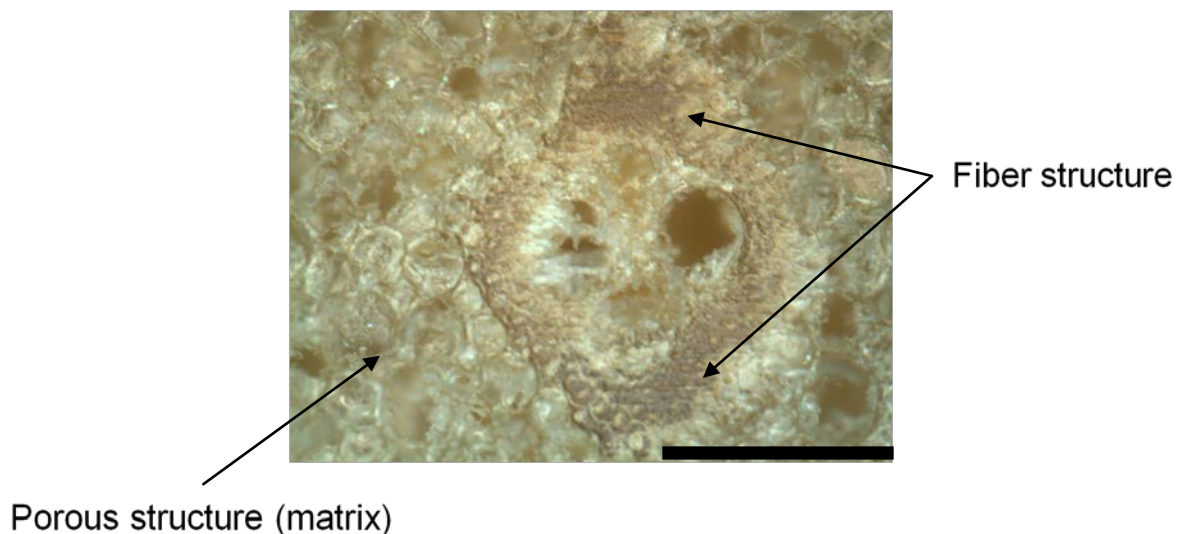


Figure 2: Basic microstructure of ADL with a scale bar of 20 microns.

Mechanically the material can be regarded as orthotropic with three symmetry directions including longitudinal, tangential and radial [2], as observed in Figure 3. Fibers are aligned in the longitudinal direction and contribute primarily to bending stiffness. Reeds are machined in this direction such that the fibers are aligned along the length of the final geometry. These directions can be seen in Figure 3, where a finished reed would be machined from the cane wall parallel to the axial direction. ADL is also a viscoelastic material that exhibits internal losses when subjected to mechanical and vibrational loads/excitation. These losses can be related to material damping through the complex Young's modulus, which can be measured through independent analysis of stress and strain waveforms. Losses are important as they contribute to

the time-varying behaviour of reeds, their deterioration and the efficiency with which tip vibrations respond to pressure waves in the air column.

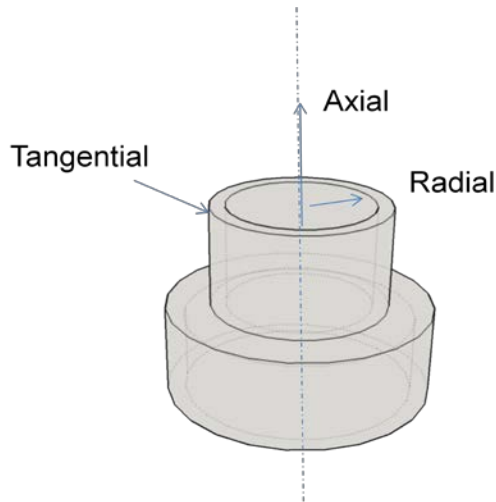


Figure 3: Primary directions in ADL

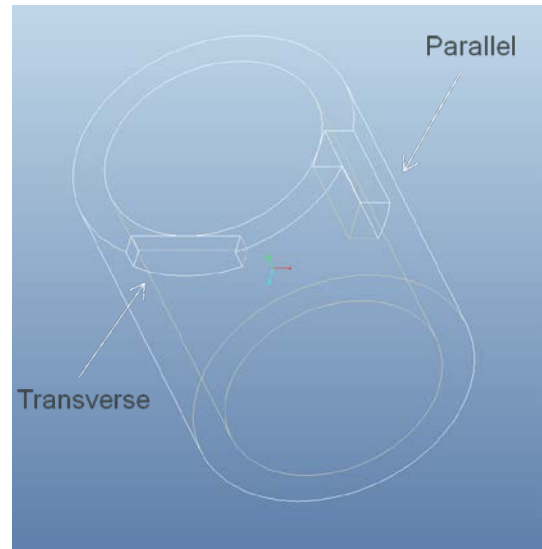


Figure 4: Geometry of test specimens

### 3.0 Experimental Details

#### 3.1 Materials

Compressive testing samples were machined from raw ADL material supplied by a reed manufacturer. Given the symmetry of ADL it was desirable to obtain specimens with fibers aligned both parallel and perpendicular to the loading axis (i.e., longitudinal and tangential directions). The geometry of the specimens was in the form of a prismatic bar and adapted from the ASTM standard for compressive samples [4] such that the slenderness ratio was maintained while working within the limits of the material (the wall thickness of raw ADL was less than 10mm). All accounted for, there were 4 specimens comprised of 2 parallel and 2 perpendicular units. Samples were conditioned at 37°C and ambient laboratory humidity (30% RH) for 24 hours prior to testing. A schematic of the sample cut-outs from the ADL cross-section is provided in Figure 4. Sample dimensions are also provided in Table 1.

Table 1: Dimensions of test specimens (mm)

<i>Specimen</i>	<i>Length</i>	<i>Width</i>	<i>Thickness</i>
<b>Longitudinal</b>	18.12	5.35	2.25
<b>Transverse</b>	14.2	5.35	2.1

### 3.2 Testing setup

#### 3.2.1 Initial characterization

Material samples were fitted with Vishay strain gauges (+/- 3%) aligned with the long-axis of the sample using a catalyst activated epoxy adhesive and subjected to cyclic compressive loading (i.e., measured strains were within the loading plane). Cyclic loading was completed using a pre-load of 100N followed by sinusoidal stress-wave input with peak amplitudes of 150 to 50N, fully compressive. For transverse specimens these values were reduced to a 50N preload and peak amplitudes of 75 to 25N. A frequency of 0.5Hz was selected for testing and measurements were recorded for 50 cycles. Measures of stress were obtained through the loading stage load cell (ADMET 2kN microtester, Figure 5) and output strain waveforms were measured through the strain gauge output signal (8Hz sampling). Samples were tested initially to observe potential inherent stress-strain phase lag differences between the specimens.

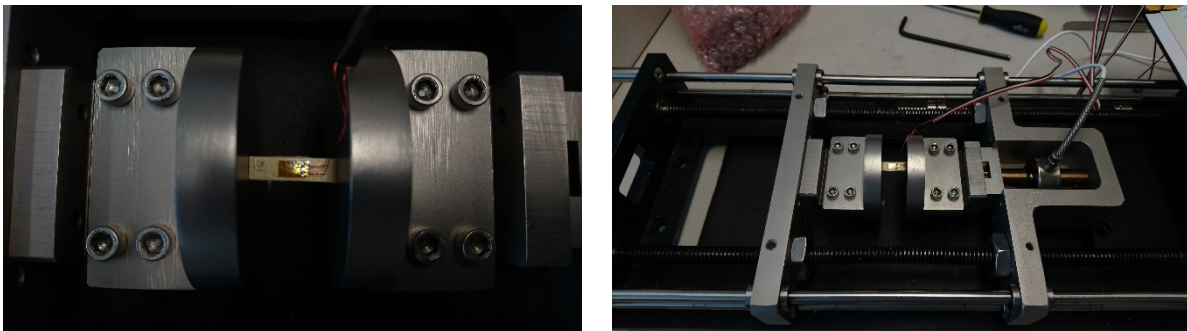


Figure 5: Stress-strain phase lag setup illustrating sample positioning and strain signal acquisition.

#### 3.2.2 Forced-vibrational loading

Simulation of in-vivo loading was completed on each of the samples using a B&K handheld exciter (Figure 6) at frequencies of 150Hz and 440Hz to simulate alto saxophone playing conditions. Specimens were rigidly mounted to a fixture and cantilevered using the exciter as a point load. Each specimen was driven at its selected frequency for a period of 3 hours. This was selected to determine if reeds experience a “break-in” period, as is often referred to by musicians. Each sample was reintroduced to the conditioning chamber after testing to ensure variability introduced through environmental effects was minimized. Tests were completed at stable ambient laboratory conditions of 24°C and 30% relative humidity.

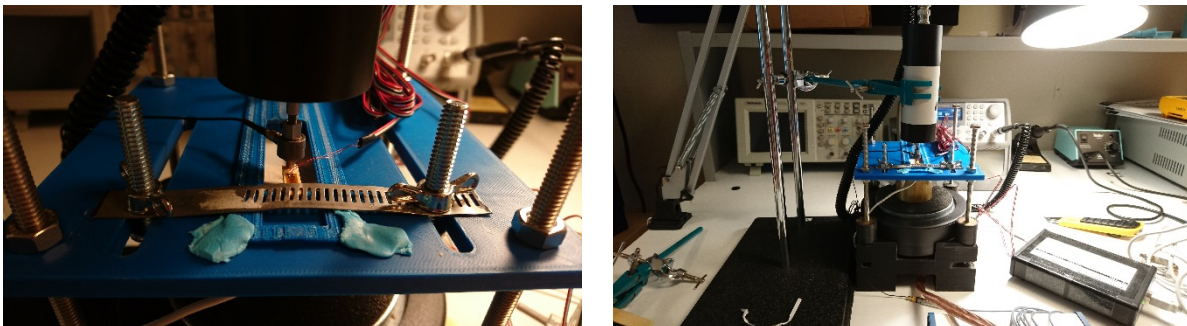


Figure 6: Vibrational exciter and cantilevered sample setup.

### 3.2.3 Microstructure

The microstructure of each sample was analyzed under optical microscope to quantify important features. These microstructural features included the average fiber size, quality of the fiber-matrix interface (qualitatively) and the existence of observable defects such as cracks and non-continuous pores. Image analysis was performed using a standard microscopy suite.

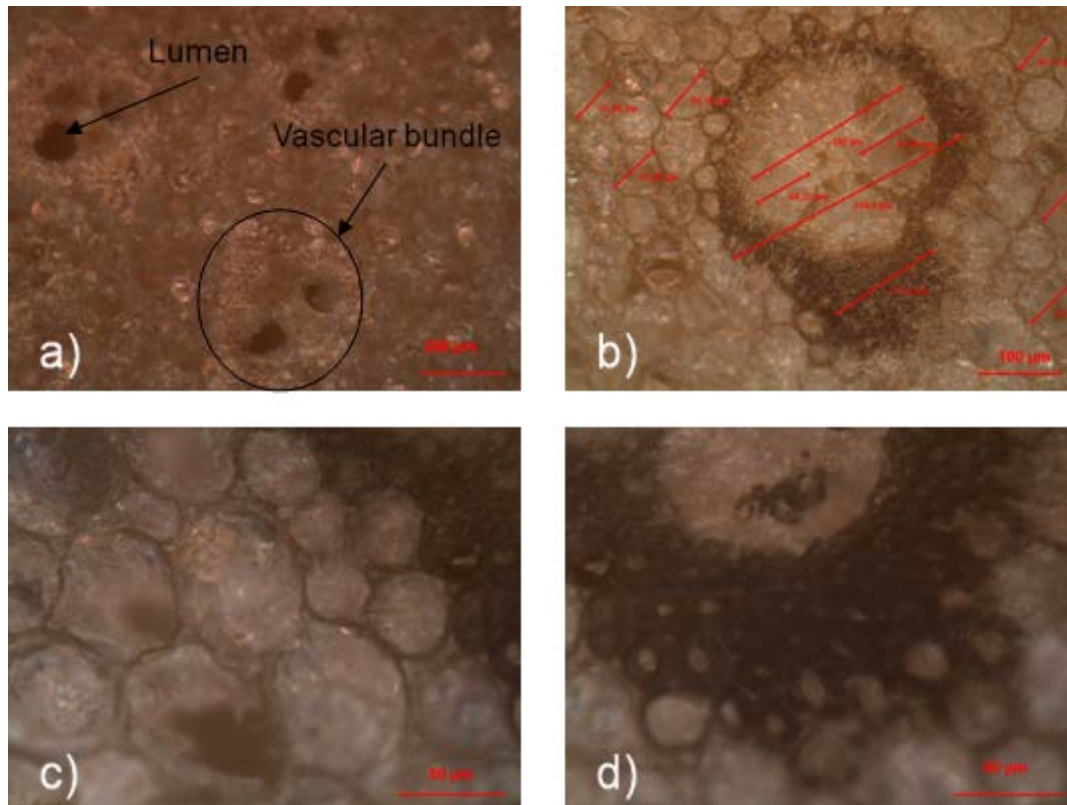


Figure 7: a) Typical microstructure of ADL illustrating vascular bundles and lumen vessels, b) analysis of a vascular bundle and surrounding area, c) structure of the parenchyma matrix and d) solid fiber material surrounding the vascular bundle.

### 3.2.4 Post-vibrational testing

Compressive testing of samples post-vibration was completed in an identical manner to that of the initial characterization phase. Both initial characterization and post-vibration characterization tests were only run once per sample to prevent slowly-relaxing internal stresses from contributing to subsequent trials.

## 4 Results

Experimental results are provided in several of the figures below, where material losses and complex moduli are computed from analysis of the obtained stress-strain signals. Stress-strain phase lag was evaluated as a loss angle (in degrees) representing the phase shift between each of these independently measured waveforms. This is typical of rheological analysis and is given as:

$$\sigma = \sigma_o \sin \omega t \quad (1)$$

$$\epsilon = \epsilon_o \sin(\omega t - \delta) \quad (2)$$

where the stress and strain functions depend on the amplitude of the input and the strain function contains a loss term,  $\delta$ , given by the phase difference between each waveform.

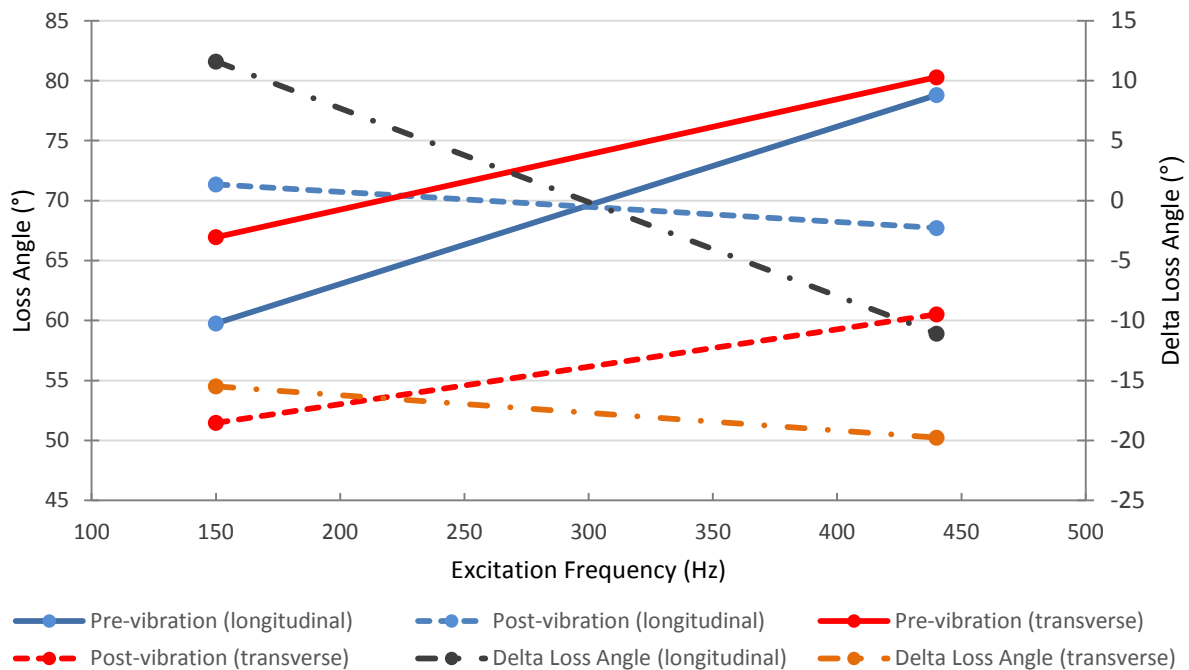


Figure 8: Stress-strain phase lag from test specimens.

Changes in the shear loss modulus,  $G''$ , are provided in Figure 9 and given as:

$$G'' = \frac{\sigma_o}{\epsilon_o} \sin \delta \quad (3)$$

where this value represents the magnitude of the complex component within the stress-strain relationship. The loss modulus is indicative of the out-of-phase viscous component of oscillatory flow.

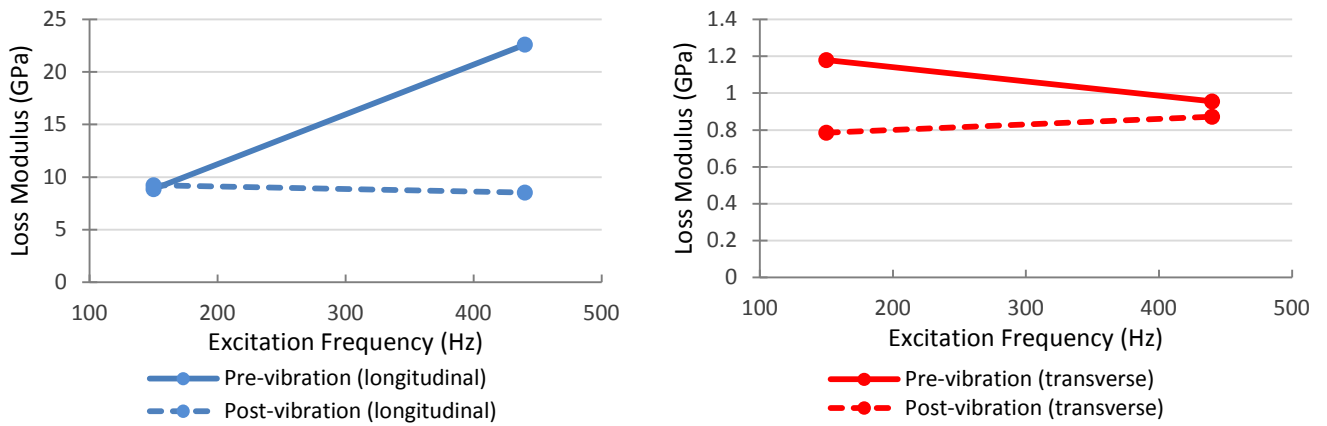


Figure 9: Left: Loss modulus of longitudinal samples. Right: Loss modulus of transverse samples.

Quantification of microstructural properties was completed at several magnifications and the results averaged for each specimen to produce results representative of the entire cross-section. Results are shown in Figure 10. These features are important to the mechanical properties of ADL and have been shown to be important to the musical performance of the reed [5].

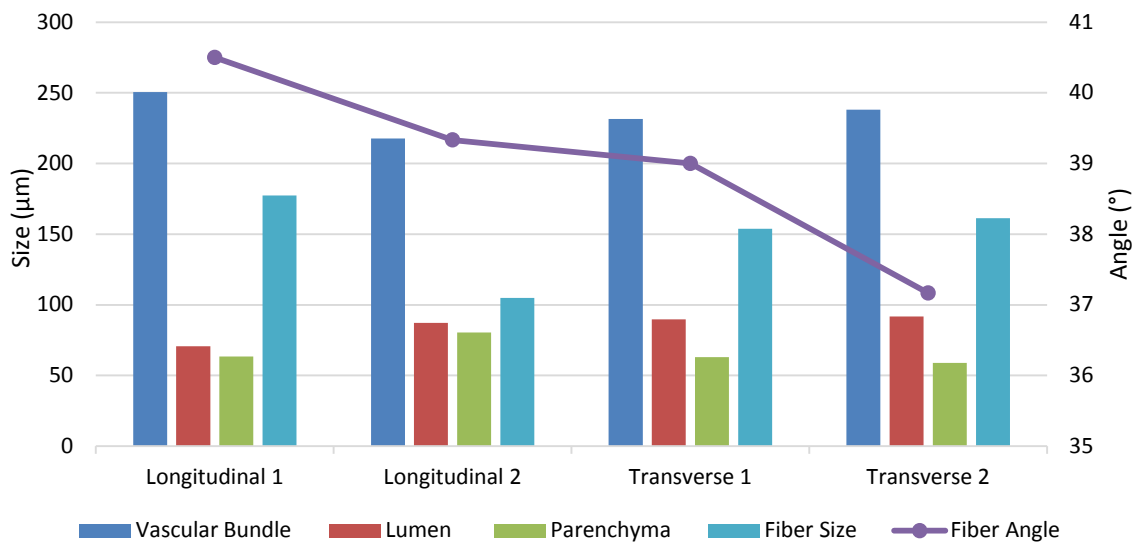


Figure 10: Microstructural parameters for each of the investigated specimens.

The loss angle is an important parameter to quantify as it is directly related to the logarithmic decrement of freely vibrating materials. Both values can be used as a measure of internal

friction [6] representing energy loss within the material (i.e., it is a material property) manifested through internal heat generation.

## 5 Discussion

From the results presented it was observed that samples exhibited changes in loss behaviour after vibration. The loss angle of each sample decreased after excitation, except for the longitudinal sample vibrated at 150Hz. This decrease in loss angle means that overall elasticity is increasing in the material. Although further investigation is required, this is likely a result of compression within the parenchyma matrix causing a reduction in overall porosity. When considering the 150Hz longitudinal sample, observations of vascular bundle size and lumen diameter within the microstructure show that this specimen deviates from the other three samples, with the highest bundle size and smallest lumen size. Further analysis of changes in loss angle before and after excitation degradation was performed by comparing delta loss angle (post-test versus pre-test) with several microstructural quantities. Figure 11 illustrates these findings.

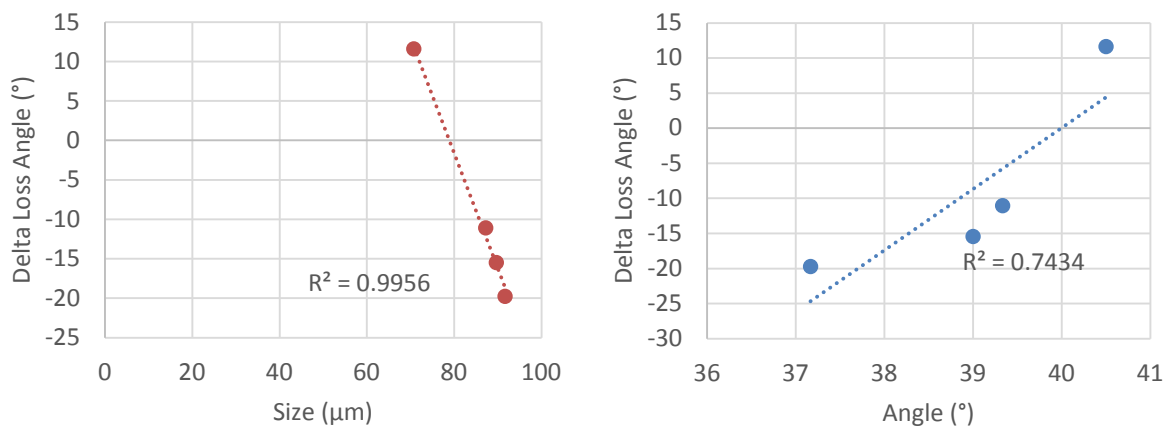


Figure 11: Left: Change in loss angle and lumen diameter. Right: Change in loss angle and orientation of fiber bundles.

The dependency on fiber orientation may indicate that more favourably aligned fibers are able to provide a larger level of load sharing with the matrix and thus contribute to more elastic behaviour after vibration. Here favourably aligned fibers refer to those that have a smaller angle and are more axially aligned. Samples were subjected to the same cantilevered strain upon application of the vibratory signals. This strain level ( $600\mu\epsilon$ ) was selected from in-vivo measurements of alto saxophone reeds as it is representative of musician average embouchure pressure. Preloads and strain wave amplitudes were reduced for transverse samples due to the large anisotropy in elastic moduli of ADL. Also worthy of note is the difference in sinusoidal stress and strain wave amplitudes between the longitudinal and transverse specimens. These values are provided in Table 2 and further illustrate the anisotropy present in ADL and provide an explanation for the increase in loss angle observed for transverse specimens.

Table 2: Oscillatory peak stress and strain for each specimen

Specimen	Peak Strain Amplitude ( $\mu\epsilon$ )	Peak Stress Amplitude (MPa)
Longitudinal 150Hz	900	4.38
Longitudinal 440Hz	1100	5.07
Transverse 150Hz	4000	2.00
Transverse 440Hz	4000	2.00

## 6 Conclusions and Future Work

A study was conducted to determine the material damping properties of a woodwind cane through the analysis of the loss angle. It was found that the loss angles decrease with specimen exposure to vibrational excitation for all but one of the samples tested. Differences in loss angle after vibrational loading are attributed to the size and orientation of fiber bundles in the microstructure. It is also noted that transverse specimens exhibit larger loss angles, likely a result of larger load sharing in the parenchyma matrix.

Future work will consider the in-vivo strains of reeds in order to better understand the mechanical and vibrational extremes that the material is under during playing. Frequency dependency of the loss angle should also be analyzed in order to better understand the validity of assuming linear viscoelasticity. Further testing at more excitation frequencies should elucidate a frequency range over which changes in loss angle occur more rapidly. More rigorous statistical analysis of microstructural features using a larger sample set will also be completed.

## Acknowledgments

The authors would like to acknowledge CIRMMT for the generous support of this research.

## References

- [1] P. Picart, J. Leval, F. Piquet, J. P. Boileau, T. Guimezanes, and J. P. Dalmont, "Study of the Mechanical Behaviour of a Clarinet Reed Under Forced and Auto-oscillations With Digital Fresnel Holography," *Strain*, vol. 46, no. 1, pp. 89–100, 2010.
- [2] E. Obataya and M. Norimoto, "Acoustic properties of a reed (*Arundo donax* L.) used for the vibrating plate of a clarinet," *The Journal of the Acoustical Society of America*, vol. 106, no. 2, pp. 1106–1110, Aug. 1999.
- [3] S. Amada and R. S. Lakes, "Viscoelastic properties of bamboo," *Journal of Materials Science*, vol. 32, no. 10, pp. 2693–2697, May 1997.
- [4] ASTM 03.01, International Standard E9-09: *Standard Test Methods of Compression Testing of Metallic Materials at Room Temperature*, USA, DOI: 10.1520/E0009-09, 2012.
- [5] P. Kolesik, A. Mills, and M. Sedgley, "Anatomical Characteristics Affecting the Musical Performance of Clarinet Reeds Made from *Arundo donax* L. (Gramineae)," *Ann Bot*, vol. 81, no. 1, pp. 151–155, Jan. 1998.
- [6] Introduction to Internal Friction: Terms and Definitions," in *Internal Friction in Metallic Materials*, Springer Berlin Heidelberg, 2007, pp. 1–10.